MATHEMATICAL BIOSCIENCES
AND ENGINEERING
Volume **9**, Number **2**, April **2012**

doi:10.3934/mbe.2012.9.413

pp. **413–430**

THE IMPACT OF SCHOOL CLOSURES ON PANDEMIC INFLUENZA: ASSESSING POTENTIAL REPERCUSSIONS USING A SEASONAL SIR MODEL

Sherry Towers*, Katia Vogt Geisse*†, Chia-Chun Tsai⋆
Qing Han* and Zhilan Feng*

*Department of Mathematics, Purdue University, West Lafayette, IN 47907, USA
⋆Department of Forestry and Natural Resources, Purdue University
West Lafayette, IN 47907, USA
†Profesor Asociado a la Facultad de Ingeniería y Ciencias de la Universidad Adolfo Ibáñez

(Communicated by Jia Li)

Abstract. When a new pandemic influenza strain has been identified, mass-production of vaccines can take several months, and antiviral drugs are expensive and usually in short supply. Social distancing measures, such as school closures, thus seem an attractive means to mitigate disease spread. However, the transmission of influenza is seasonal in nature, and as has been noted in previous studies, a decrease in the average transmission rate in a seasonal disease model may result in a larger final size. In the studies presented here, we analyze a hypothetical pandemic using a SIR epidemic model with time- and age-dependent transmission rates; using this model we assess and quantify, for the first time, the the effect of the timing and length of widespread school closures on influenza pandemic final size and average peak time.

We find that the effect on pandemic progression strongly depends on the timing of the start of the school closure. For instance, we determine that school closures during a late spring wave of an epidemic can cause a pandemic to become up to 20% larger, but have the advantage that the average time of the peak is shifted by up to two months, possibly allowing enough time for development of vaccines to mitigate the larger size of the epidemic. Our studies thus suggest that when heterogeneity in transmission is a significant factor, decisions of public health policy will be particularly important as to how control measures such as school closures should be implemented.

1. **Introduction.** Influenza, a seasonal viral disease, presents a significant morbidity and mortality burden on the population, with a typical seasonal influenza epidemic in the United States killing around 40,000 people per year[12]. However, during pandemic years, this number can be much larger. Influenza pandemics occur when a human influenza A virus re-assorts with an animal influenza A virus, such as one from birds or pigs. Pre-existing immunity within the population is low to these new strains, and thus pandemics are created if the strain is highly transmissible.

Because several months are needed to mass-produce vaccines once a new pandemic strain has been identified, mitigation strategies must be considered to reduce

2000 *Mathematics Subject Classification.* Primary: 92D30.
Key words and phrases. Pandemic influenza, epidemic model, dynamic systems.

influenza-related infections, such as pharmaceutical interventions (vaccination, antiviral drugs), and/or social distancing measures, such as school or workplace closures. In a pandemic situation school closures tend to be particular attractive in light of the high morbidity of pandemic influenza strains in children and young adults, compared to seasonal influenza which has highest morbidity in infants and the elderly.

While school closures are a relatively easy intervention to implement compared with pharmaceutical methods, they can nevertheless cause significant social and economic disruption to the community. For instance, the estimated potential economic cost of blanket school closure in U.S. is 2.7 million dollars per 1000 population per week, or $\sim 6\%$ GDP[30]. There thus remains substantial debate over the impact of school closure as a mitigation strategy during an influenza pandemic.

Reference [7] reviews multiple studies of past data that assess the effect of school closures on the spread of influenza. While several appear to find that closures of several weeks are sufficient to reduce the attack rate, it must be cautioned that most of these studies compare the attacks rate over a short period immediately during and after the school closure to the attacks rate immediately before (e.g.; they do not examine the longer-term effect of the school closure). The longer-term impact of such school closures has thus been poorly studied.

There have also been many modeling studies to assess the efficacy of school closures and other intervention strategies on the spread of pandemic influenza[10, 14, 17, 18, 19, 20, 23, 24, 28]. All predict that school closures of at least several weeks generally have notable impact on the course of the epidemic (as long as they do not occur too late in the pandemic), and none find that school closures negatively impact the course of the pandemic.

However, these models do not take into account the seasonality of influenza; influenza is known to be more transmissible in the winter months in temperate regions than in tropical regions, in part due to seasonality of host health (susceptibility to infection) and environmental effects on the transmissibility of the virus[1, 8, 11, 25, 26]. School closures temporarily reduce the transmission rate of the virus, and thus reduce the average transmission rate taken over the course of the year. As has been shown in References [4] and [32], reduction of the average transmission rate in a seasonal model may result in an increased epidemic final size. Thus seasonality is important to take into consideration when considering interventions such as school closures; a school closure applied during the spring/summer wave of a pandemic, which occurs during relatively unfavorable time of year when transmissibility is waning, may indeed reduce the peak of that wave, but only to supply a much greater number of susceptible individuals when school finally reconvenes in autumn, which is a more favorable season for influenza transmissibility. If the virus is still circulating in the population at that time, a large autumn pandemic could potentially result, instead of the smaller summer epidemic that would have occurred (and burned itself out) if school closures had not taken place. This could explain the curious phenomenon observed in the 1918 pandemic, where Connecticut cities that kept schools open reported lower death rates compared to Connecticut cities that closed their schools[35].

In the studies presented here we examine the seasonality of influenza with a Susceptible, Infected, Recovered (SIR) mathematical model with a periodically forced transmission rate to reflect the fact that the transmissibility of influenza is higher

in the winter than in summer. We extend this seasonal model to include age-heterogeneity, with two age classes representing children and adults.

Using this model, we study the impact of reduced contact between children during school closures on the final size of a pandemic influenza outbreak under various scenarios of length of school closure and closure trigger conditions. We show that when transmissibility is seasonal in nature, school closures do not always have the desired effect of reducing the size of the epidemic, and in fact can sometimes make the epidemic substantially larger than it might otherwise have been. We also show that the average peak timing of seasonal epidemics is delayed by school closures, sometimes significantly so. Indeed, as we will show, closures that result in significantly increased final size also tend to significantly delay the average peak time; an outcome which may be desirable if vaccines can be produced in time to ameliorate the associated increase in the final size. These results have obvious implications for public health policy, and underline the role that mathematical models can play in helping to assess disease intervention strategies.

2. **Model.** One of the simplest epidemiological models is the so called SIR model[2], in which we model the number of susceptible (S), infected (I), and recovered (R) people in the population using the deterministic ordinary differential equations:

$$\begin{aligned} S' &= -\beta(t)SI/N \\ I' &= \beta(t)SI/N - \gamma I \\ R' &= \gamma I, \end{aligned} \tag{1}$$

where $1/\gamma$ is the average infectious period (assumed here to be three days for influenza[9]), $\beta(t)$ is the transmission rate, and population size $N = S + I + R$. Because we will be considering pandemics of very short duration relative to human population dynamics, we do not include vital dynamics in the models we discuss here.

In most simple epidemiological models, $\beta(t) = \beta$ is assumed to be a constant. However, for diseases such as influenza, seasonal variation in the transmission rate is important to consider[3, 4, 13, 32, 34]. Any periodic function can be expressed as a sum of harmonic terms. In this analysis we model periodicity of transmission due to seasonal effects on host health and seasonal environmental effects (such as temperature, humidity, etc) using the first order harmonic

$$\beta(t) = \beta_0 \left[1 + \epsilon \cos(2\pi\omega t)\right], \tag{2}$$

where the period is $1/\omega = 365$ days, β_0 is the average transmission rate over one period, and ϵ is the degree of seasonal forcing. We define the β function given in Equation (2) to have its maximum at the beginning of a calendar year. The results of this analysis can be easily generalized to include a phase if it is believed that influenza transmission peaks at some other time of year, but inclusion of a phase does not affect the overall conclusions of the study.

The time of introduction of the virus to the population, t_0, is a parameter of the seasonal model when the transmission rate is expressed in a periodic form, and the final size and shape of the epidemic curve (including how many peaks the epidemic exhibits) can depend quite strongly on this parameter (whereas for constant β the final size and shape are independent of t_0, and the epidemic curve can exhibit only one peak in the absence of vital dynamics in the model)[3, 4, 13, 32]. We will discuss

in a moment how we add into the model the additional seasonality due to periodic school closures.

TABLE 1. Definition of symbols and parameter values used in simulations

Variables	Definition	Value (range)
$S(t)$	# of susceptible individuals at time t	
$I(t)$	# of infectious individuals at time t	
$R(t)$	# of recovered individuals at time t	
Parameters		
γ	Recovery rate	$1/\gamma = 3$ days[9]
ϵ	oscillation magnitude of the transmission rate, $\beta(t)$	0.10
t_0	time of introduction of the virus to the population	Varied
f	Fraction population under 19 years of age	0.29[33]
N	Population size	$10,000,000$ (results of study not sensitive to N)
C_{11}	Number of child-to-child contacts per day	13
C_{12}	Number of child-to-adult contacts per day	3
C_{21}	Number of adult-to-child contacts per day	2
C_{22}	Number of adult-to-adult contacts per day	10
$\mathcal{R}_0$	Reproduction number of pandemic influenza	1.7
β_0	Average transmission rate	$\mathcal{R}_0\gamma/14$ (see Equation 6)
p	scale factor for child-to-child contact during school closure	0.50
f^{crit}	Trigger value of prevalence for closure	Varied
t_{close}	Beginning time of school closure	Varied
L_{close}	Duration of school closure	Varied

In order to study age-targeted disease intervention strategies, such as school closures, we expand the model in Equations (1) to include age heterogeneity, with mixing between $n = 2$ different age-stratified classes representing children less than 19 years of age, and adults:

$$\begin{aligned} S_i' &= -\beta(t) S_i \sum_{j=1}^{n} C_{ij} I_j / N_j \\ I_i' &= \beta(t) S_i \sum_{j=1}^{n} C_{ij} I_j / N_j - \gamma I_i \\ R_i' &= \gamma I_i, \end{aligned} \tag{3}$$

where the population size, N, is $N = \sum_i N_i = \sum S_i + \sum I_i + \sum R_i$. The matrix C_{ij} is known as the *contact matrix*, and is the average number of contacts made per day by an individual in class i with an individual in class j. In this analysis we determine C_{ij} using physical contact data from the detailed sociological contact

survey data of Mossong *et al* [29], where participants kept daily diaries recording the length and nature of their contacts. We do this using the methods outlined in Reference [27]. The resulting contact matrix is shown in Table (1).

We implement school closures in our model with factors multiplying the elements of the contact matrix to simulate social distancing between members of the population during closures. In a study of the effect of school closures in France on the spread of seasonal influenza, Cauchemez *et al* concluded that school closures appear to result only in reduced contact rate patterns between children (they find the contacts of children reduce by a factor of 25% during holidays), and that the contact patterns of adults remain essentially unchanged[8]. We thus include school closures in our model as a factor, $p(t)$, multiplying C_{11} only. Namely,

$$\begin{aligned} S_1' &= -\lambda_1(t)S_1 \\ S_2' &= -\lambda_2(t)S_2 \\ I_1' &= \lambda_1(t)S_1 - \gamma I_1 \\ I_2' &= \lambda_2(t)S_2 - \gamma I_2 \\ \lambda_1(t) &= \beta(t)\left[\, p(t)\, C_{11}I_1/N_1 + C_{12}I_2/N_2\right] \\ \lambda_2(t) &= \beta(t)\left[C_{21}I_1/N_1 + C_{22}I_2/N_2\right], \end{aligned} \tag{4}$$

with initial conditions at the time of introduction, t_0, of the infection into the population

$$\begin{aligned} S_1(t_0) &= fN - 1, \\ S_2(t_0) &= (1-f)N - 1 \\ I_1(t_0) &= 1 \\ I_2(t_0) &= 1 \\ R_1(t_0) &= 0 \\ R_2(t_0) &= 0, \end{aligned} \tag{5}$$

where f is based on the demographics of the population. In the U.S. population, the fraction of people under the age of 19 is $f = 29\%$[33]. We assume the scale factor $p(t) = 1$ when school is in session, and $p(t) = 0.5$ when school is closed, unless otherwise specified.[1] In this way we implement in the model not only extra school closures designed to intervene in the spread of disease, but also regularly scheduled school holiday closures. In this analysis the start time of disease-intervention school closures is determined by trigger conditions, determined by the prevalence of the disease in the population, f_{crit}. We explore the efficacy of the school closure as a disease intervention strategy as a function of the trigger condition, and the length of the closure, L_{close}.

Estimation of ϵ, the seasonal forcing term of $\beta(t)$ must be considered; it is known that seasonality of influenza is due to *both* periodicity in school closures, *and* environmental effects on host health and virus transmissibility, however the relative contribution of these to the overall disease dynamics is not well know. However, data and modeling studies indicate that values of 0.25 to 0.35 appear to be reasonable estimates for the overall seasonal variation in transmission due to the effects of both $\beta(t)$ and $p(t)$ combined[3, 15, 31]. From the studies of Cauchemez *et al*, we

[1] We assume a somewhat greater reduction of contacts between children than that observed by Cauchemez *et al* during school holidays, because we wish to replicate the extra social distancing more likely to be experienced during a pandemic situation.

know that the value $p(t)$ only reduces the contact rates of children by 25% during school holidays/closures, not the entire population, thus the contact rate of the entire population is reduced by around 12%. We thus assume in our studies that the remaining seasonal variation is incorporated in the $\beta(t)$ function, and is on the order of $\epsilon = 0.10$. We will use this value in this analysis, unless otherwise specified.

The parameters of the model are shown in Table (1).

3. **Results.** In this section we study the school closure model in Equations (4) under two scenarios:

1. Transmission rate $\beta(t)$ =constant.
2. Periodic transmission rate.

We show that the first scenario always improves the outcome of the epidemic, but that this is not always necessarily the case for the latter.

3.1. **The case of constant transmission rate.** In epidemiological models, one of the most important quantities is the *basic reproduction number*, denoted by $\mathcal{R}_0$. It is the average number of secondary infections produced by one infected individual during his/her entire period of infection in an entirely susceptible population. If $\mathcal{R}_0$ falls below 1, the disease fails to spread within the population, and the epidemic dies out. This number determines whether there will be an epidemic outbreak when a small number of cases are introduced in the population, and how severe the outbreak will be in the absence of any programs of disease control and prevention.

For constant $\beta(t) = \beta_0$, the basic reproduction number of the system in Equations (3) is

$$\mathcal{R}_0 = \frac{\beta_0}{2\gamma}\left[(C_{11}+C_{22}) + \sqrt{(C_{11}-C_{22})^2 + 4C_{12}C_{21}}\right]. \tag{6}$$

When control measures are implemented, the corresponding quantity is termed the *control reproduction number* and denoted by $\mathcal{R}_c$ (c for control). One of the objectives of control programs is to reduce $\mathcal{R}_c$ to below 1, and the best strategies is usually the one that reduces $\mathcal{R}_c$ the most, given the constraints of the resources at hand. However, when model parameters are varying with time, as they are in the model of Equations (4) because of the time varying scale factor $p(t)$, the analytical results for $\mathcal{R}_c$ such as reproduction number described in Equation (6) will be difficult to obtain; $\mathcal{R}_c$ cannot be obtained simply from the average of $\beta(t)$ over the period[4, 5, 6]. In this analysis we thus rely on numerical studies to examine how control measures affect the spread of disease.

We focus on three important measures in assessment of the effect of a school closure program: (i) peak size of the epidemic curve (the maximum number of infections during the course of a pandemic); (ii) peak time (the time at which the peak occurs); and (iii) final size (the total number of infected by the end of a pandemic). Both the peak size and the peak time can be observed from the epidemic curve, while the cumulative infection curve shows the final size. Control strategies should aim to lower the peak size to reduce the burden on health care facilities (lest the demand exceed the supply), lower the final size of the epidemic to reduce morbidity and mortality, and delay the timing of the peak(s) to provide time for preparation of response measures, such as vaccines.

In Figure (1) we show the percent relative difference in final size of an epidemic versus the time of the start of school closure, as predicted by the model in Equations (4), for prevalence trigger conditions for the school closure, $f_{\text{crit}} = 0.001$ and

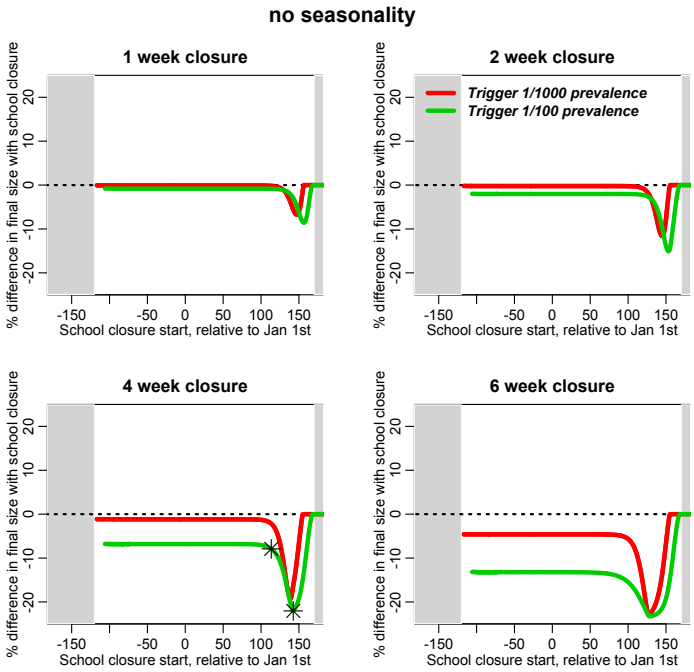

FIGURE 1. The percent relative difference in final size of a pandemic versus the time of the start of school closure, for prevalence closure trigger conditions $f_{\text{crit}} = 0.001$ and 0.01, and constant transmission rate (i.e.; no seasonality). The relative difference is the final size with closure, minus the final size without closure, divided by the final size without closure. We show this for four different closure lengths $L_{\text{close}} = 1$ week, 2 weeks, 4 weeks, and 6 weeks for a pandemic with $\mathcal{R}_0 = 1.7$, $\epsilon = 0$, and reduction in contacts between children during closure of $p = 0.50$. The grey areas indicate regularly scheduled school holidays.
To examine further the epidemic dynamics behind these results, in Figure (4) we show the behavior of the epidemic curves before and after school closure for the points represented by the asterisks.

0.01[2]. The relative difference is the final size with closure minus the final size without closure, divided by the final size without closure. We show this for four different closure lengths $L_{\text{close}} = 1$ week, 2 weeks, 4 weeks, and 6 weeks for a pandemic flu-like illness with $\mathcal{R}_0 = 1.7$, $\epsilon = 0$, and reduction in contacts between children during closure of $p = 0.50$. Note that some closure scenarios result in a significant reduction in the size of the epidemic, but at worst cause no change in the final size.

It is also important to consider whether or not the peak of the epidemic was delayed. When we consider the case of seasonality of transmission, we will find

[2]Prevalence trigger condition $f_{\text{crit}} = 0.1$ was tried as well, but no epidemic curve had a large enough peak to meet the condition when the transmission rate was constant.

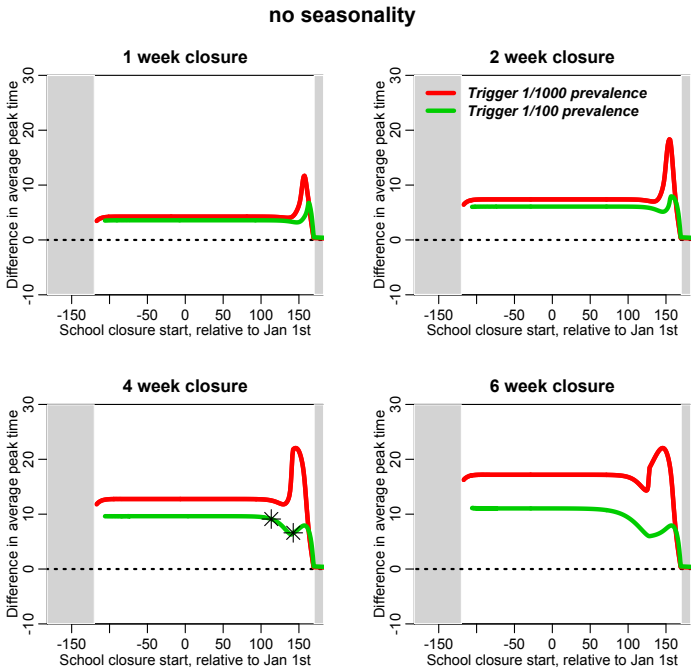

FIGURE 2. The difference the average peak time of the pandemic before and after school closure, $(\mu^{\text{peak}}_{\text{after}} - \mu^{\text{peak}}_{\text{before}})$, versus the time of the start of school closure, for prevalence closure trigger conditions $f_{\text{crit}} = 0.001$ and 0.01, and constant transmission rate (i.e.; no seasonality). We show this for four different closure lengths $L_{\text{close}} = 1$ week, 2 weeks, 4 weeks, and 6 weeks for a pandemic with $\mathcal{R}_0 = 1.7$, $\epsilon = 0$, and reduction in contacts between children during closure of $p = 0.50$.
In Figure (4) we show the behavior of the epidemic curves before and after school closure for the points represented by the asterisks.

that multiple peaks can occur in the epidemic curve, thus we must define a statistic that indicates when the average peak time of the epidemic occurred. If we have prevalence measurements at k consecutive time points, we can calculate this average peak time of the epidemic as

$$\mu^{\text{peak}} = \frac{\sum_{i=1}^{k} t_i I_i}{\sum_{i=1}^{k} I_i}. \tag{7}$$

One goal of social distancing measures, such as school closures, is to shift the peak time of the epidemic to be later, to allow more time for mass-production of vaccines and other pharmaceutical interventions. In Figure (2) we show the difference in μ^{peak} for the prevalence trigger and school closure length conditions described above. Note that some closure scenarios result in a delay of the average peak time, but at worst cause no difference in the timing of the peak.

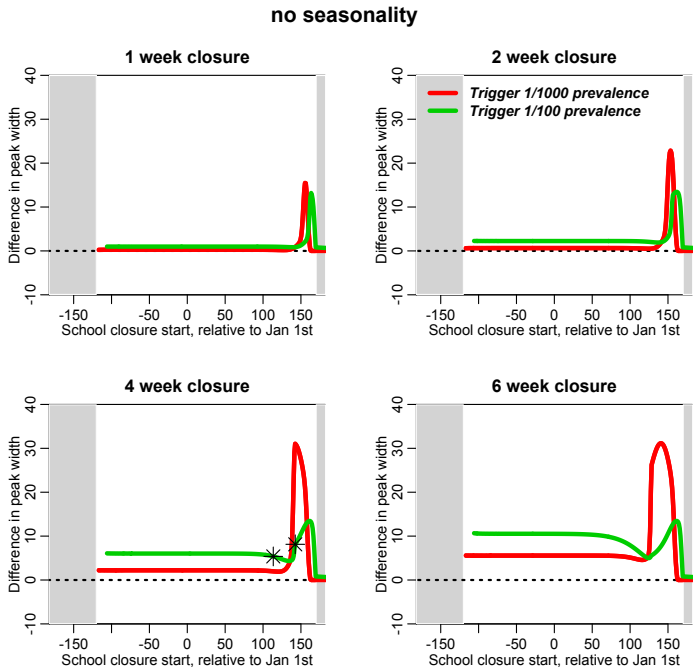

FIGURE 3. The difference the average peak width of the pandemic before and after school closure, $(\sigma^{\text{peak}}_{\text{after}} - \sigma^{\text{peak}}_{\text{before}})$, versus the time of the start of school closure, for prevalence closure trigger conditions $f_{\text{crit}} = 0.001$ and 0.01 and constant transmission rate (i.e.; no seasonality). We show this for four different closure lengths $L_{\text{close}} = 1$ week, 2 weeks, 4 weeks, and 6 weeks for a pandemic with $\mathcal{R}_0 = 1.7$, $\epsilon = 0$, and reduction in contacts between children during closure of $p = 0.50$. The grey areas indicate regularly scheduled school holidays.
In Figure (4) we show the behavior of the epidemic curves before and after school closure for the points represented by the asterisks.

We can also calculate the standard deviation (width of the peak); a smaller width implies a sharper distribution, and greater average load on hospital resources near the peak. A larger width is a desirable outcome of social distancing measures. The standard deviation is calculated as

$$\sigma^{\text{peak}} = \sqrt{\frac{\sum_{i=1}^{k} \left(t_i - \mu^{\text{peak}}\right)^2 I_i}{\sum_{i=1}^{k} I_i}}. \tag{8}$$

In Figure (3) we show the difference in σ^{peak} for the prevalence trigger and school closure length conditions described above. Note that some closure scenarios result in a significant widening of the peak, but at worst make no difference in the width of the peak.

To examine further the epidemic dynamics behind these results, Figure (4) gives an example of two pandemic scenarios, one of which is a school closure triggered in

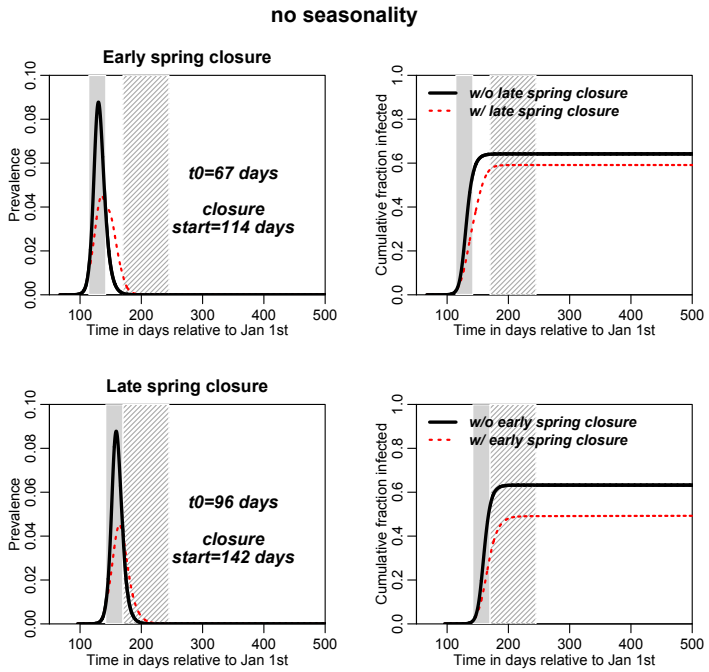

FIGURE 4. The right hand plots indicate prevalence of a pandemic versus time, when the trigger condition for the school closure is prevalence in the population of 1/100, and the transmission rate is constant (i.e.; there is no seasonality), and for school closure length of four weeks and reduction in contacts between children during closure by a factor of $p = 0.50$. The left hand plots indicate the cumulative incidence over time. In both plots the light gray area indicates the school closure, and the hatched gray area represents the regular school holiday.
In the top (bottom) scenario the closure was triggered in early (late) spring. The closure that ended just as summer vacation began resulted in maximum possible reduction of the spring wave.

early spring, and the other of which is a school closure triggered in late spring that results in a maximal reduction in final size. The former had an epidemic that peaked earlier than the latter, and the epidemic had ended before school holidays began (thus school holidays had no further impact on reducing the epidemic size). In contrast, closure that occurred during the late spring epidemic shifted the timing of the peak forward, causing it to peak just as the school holidays began, thus allowing those holidays to have a much greater impact on reducing the size of the epidemic than they otherwise would have had.

3.2. **The case of periodic transmission rate.** In this section, we examine a model where the transmission rate $\beta(t)$ has the periodic form as in Equation (2).

The basic reproduction number of a periodic disease system is not straightforward to define[4, 6, 34]. However, we note that near the beginning of the 2009 A(H1N1)

pandemic, the $\mathcal{R}_0$ of the virus was estimated to be around 1.3 to 1.7[16, 31, 36]. For simplicity, we assume these measurements occurred when $\beta(t) = \beta_0$, and then use the estimate of $\mathcal{R}_0$ to estimate β_0 using Equation (6). We assume a hypothetical pandemic flu-like illness, with $\mathcal{R}_0$ at the upper end of this range, $\mathcal{R}_0 = 1.7$. The result for β_0 is shown in Table (1).

Under the assumption of seasonal forcing $\epsilon = 0.10$, we determine how school closures of varying lengths might potentially impact the course of such a pandemic for various prevalence trigger conditions.

We begin with examination of a range of times-of-introduction of the virus to the population from $[-182, +182]$, in increments of one day, and using the model in Equations (1), we calculate the resulting epidemic curve for the case of no school closure. For each subset of parameters, we then examine the school closure model in Equations (4).

We assume a range of school closure lengths from $L_{\text{close}} = 1$ week, 2 weeks, 4 weeks, and 6 weeks, and we compare the final size of the epidemic with and without school closure. In all simulations we assume a reduction in contacts between children during closure $p = 0.50$, unless otherwise noted.

This study primarily focuses on the sensitivity of the final epidemic outcomes to the duration and timing of school closures. We do not consider pre-vaccination, and assume no pre-immunity within the population to the virus due to prior infection with related strains, similar to what would be the case in an actual pandemic situation. We consider vaccination and pre-immunity effects with a periodic SIR model in [13].

Results of the model simulations are shown in Figure (5). In the Figure we show the percent relative difference in final size of an epidemic versus the time of the start of school closure, as predicted by the model in Equations (4), for prevalence trigger conditions $f_{\text{crit}} = 0.001$, 0.01, and 0.1. We show this for four different closure lengths $L_{\text{close}} = 1$ week, 2 weeks, 4 weeks, and 6 weeks. Note that, unlike the constant transmission scenario seen in Figure (1), closures in late spring appear to detrimentally impact the pandemic, resulting in larger final size. Closures triggered in late winter or early spring appear to be most advantageous, with greatest reduction in final size. Larger prevalence trigger fractions also appear to be most advantageous in producing a greater reduction in final size, however only winter epidemics have a large enough peak to trigger a school closure if the trigger fraction is too high.

In Figure (6) we show the difference in the average peak time, μ^{peak}, for the prevalence trigger and school closure length conditions described above. Nearly all closure scenarios result in a delay of the average peak time when the closure trigger prevalence is less than 1%. The closures triggered by a high prevalence of 10% are, however, ineffective at delaying the peak. Note that although late spring closures result in significant delays in the average peak time, they also usually result in significantly increased in final size (see Figure (5)), usually because they result in the creation of an autumn wave (a scenario which we shall discuss in detail in a moment). This can still be considered advantageous if the aim of the closure is to obtain enough time to mass-produce vaccines before the bulk of the epidemic has passed; if the vaccines are implemented before the autumn peak, they can mitigate the increase in the final size brought on by the school closure.

In Figure (7) we show the difference in the peak width, σ^{peak}, for the prevalence trigger and school closure length conditions described above. Similar to what was

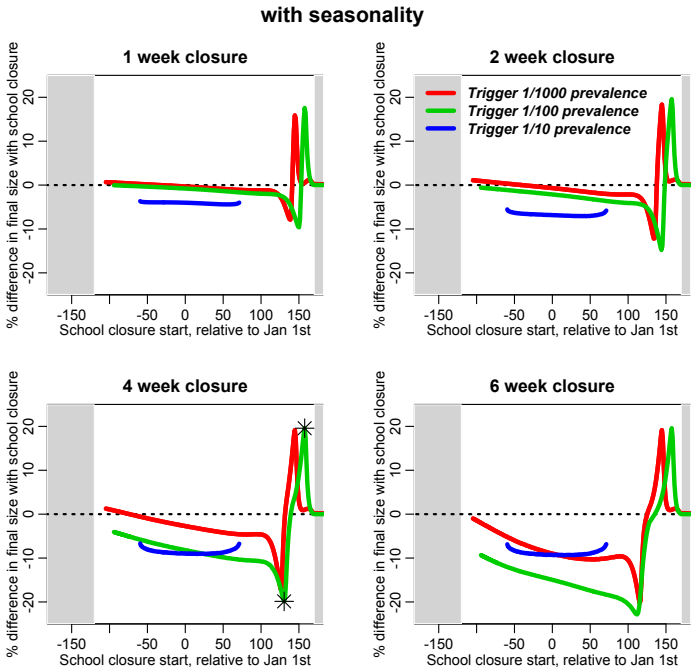

FIGURE 5. The percent relative difference in final size of a pandemic versus the time of the start of school closure, for prevalence closure trigger conditions $f_{\text{crit}} = 0.001$, 0.01, and 0.1, and seasonal forcing of the transmission rate, $\epsilon = 0.10$. The relative difference is the final size with closure, minus the final size without closure, divided by the final size without closure. We show this for four different closure lengths $L_{\text{close}} = 1$ week, 2 weeks, 4 weeks, and 6 weeks for a pandemic with $\mathcal{R}_0 = 1.7$, $\epsilon = 0$, and reduction in contacts between children during closure of $p = 0.50$. The grey areas indicate regularly scheduled school holidays.
To examine further the epidemic dynamics behind these results, in Figure (8) we show the behavior of the epidemic curves before and after school closure for the points represented by the asterisks.

noted for the average peak timing, we note that late spring closures generally result in widening of the epidemic curve, which can be considered advantageous because it lowers demand on hospital resources near the peak. However, most of those scenarios also resulted in significantly increased final sizes. The school closures caused by the high prevalence trigger of 10% had virtually no effect on the peak width, usually because the closure occurred right near the time of the peak.

To examine further the epidemic dynamics behind these results, Figure (8) gives an example of two pandemic scenarios, one of which is detrimentally impacted by school closure, and the other of which is not. The top row of plots have time of introduction of the virus $t_0 = 103$ days, and the trigger threshold of school closure when prevalence is 1/100 results in an increase in the final size of the epidemic,

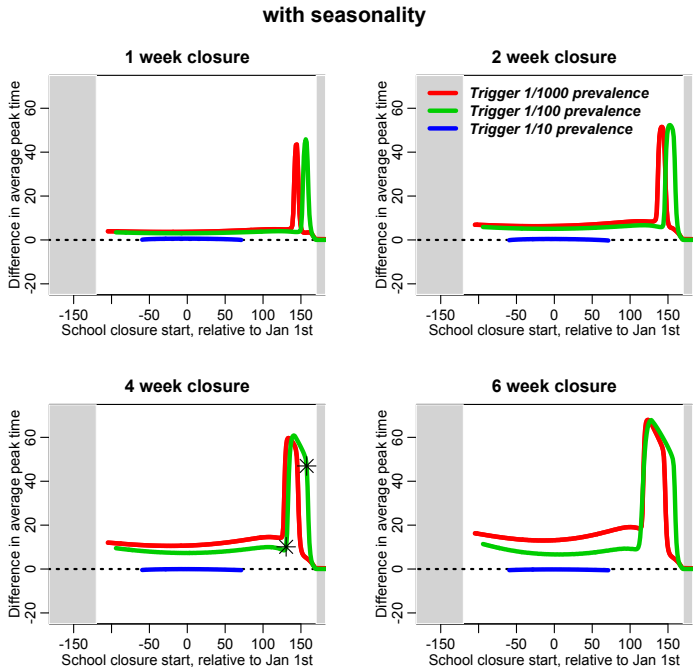

FIGURE 6. The difference the average peak time of the pandemic before and after school closure, $(\mu^{\text{peak}}_{\text{after}} - \mu^{\text{peak}}_{\text{before}})$, versus the time of the start of school closure, for prevalence closure trigger conditions $f_{\text{crit}} = 0.001$, 0.01, and 0.1, and seasonal forcing of the transmission rate, $\epsilon = 0.10$. We show this for four different closure lengths $L_{\text{close}} = 1$ week, 2 weeks, 4 weeks, and 6 weeks for a pandemic with $\mathcal{R}_0 = 1.7$, $\epsilon = 0$, and reduction in contacts between children during closure of $p = 0.50$. The grey areas indicate regularly scheduled school holidays.
In Figure (8) we show the behavior of the epidemic curves before and after school closure for the points represented by the asterisks.

and an autumn wave that otherwise would not have existed but for the school closure. This is because the school closure causes the fraction of susceptibles in the population to be larger in the fall than it would be otherwise, providing "kindling" for the epidemic to continue on into the autumn when $\beta(t)$ is again rising.

In contrast, the bottom row of plots in Figure (8) use exactly the same model parameters, except with time of introduction only 22 days earlier, $t_0 = 81$ days. There is now a reduction in the final size of the epidemic. Epidemics that are seeded earlier in the year, and thus peak earlier (and accordingly pass the prevalence trigger threshold earlier), are more likely to burn out by the end of the summer holidays with the aid of a school closure, and not produce a second autumn wave of infection.

4. **Discussion.** In this paper we presented an age-structured SIR epidemic model to study the effect of school closures on the control and prevention of pandemic influenza. A novel aspect of these studies involved our extension of the model to

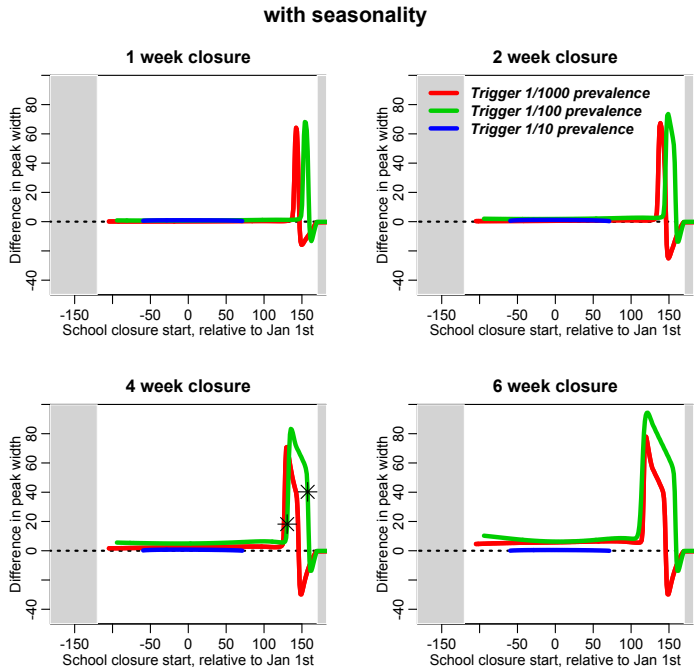

FIGURE 7. The difference the average peak width of the pandemic before and after school closure, $(\sigma^{\text{peak}}_{\text{after}} - \sigma^{\text{peak}}_{\text{before}})$, versus the time of the start of school closure, for prevalence closure trigger conditions $f_{\text{crit}} = 0.001$, 0.01, and 0.10, and constant transmission rate (i.e.; no seasonality). We show this for four different closure lengths $L_{\text{close}} = 1$ week, 2 weeks, 4 weeks, and 6 weeks for a pandemic with $\mathcal{R}_0 = 1.7$, $\epsilon = 0$, and reduction in contacts between children during closure of $p = 0.50$. The grey areas indicate regularly scheduled school holidays.
In Figure (8) we show the behavior of the epidemic curves before and after school closure for the points represented by the asterisks.

include a seasonally forced transmission rate; this model more accurately reflects the fact that the seasonality of influenza is not only due to periodicity of school closures, but also due to seasonality of host health, and environmental effects on the transmissibility of the virus. This seasonal transmission model predicts that school closure carries significant risk of making the final size of a pandemic larger if the timing of the closure occurs too late in the spring. School closures that occur earlier in the year are generally beneficial in reducing the final size of the epidemic, with the relative size of the reduction depending on the length of the closure.

Disease models with periodic transmission rates are extremely non-linear, and the final size and dynamics predicted by such models are strongly dependent upon the model parameters and initial conditions[4, 13, 32]. This can lead to interesting multi-wave dynamics, such as those observed during the 2009 and 1918 pandemics. For instance, an epidemic which begins in the population during an unfavorable time

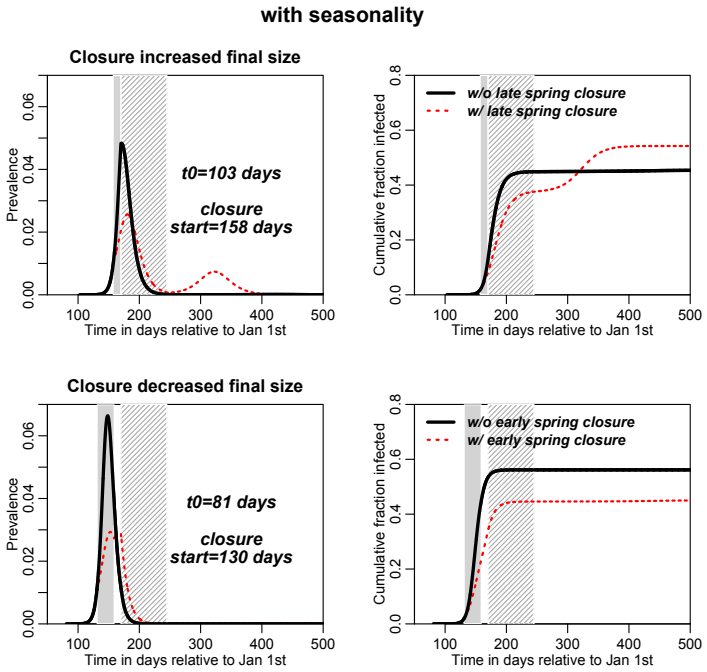

FIGURE 8. The right hand plots indicate prevalence of a pandemic versus time, when the trigger condition for the school closure is prevalence in the population of $f_{\text{crit}} = 0.01$, and the transmission rate is periodic (i.e.; there is seasonality with $\epsilon = 0.10$), and for school closure length of four weeks and reduction in contacts between children during closure by a factor of $p = 0.50$. The left hand plots indicate the cumulative incidence over time. In both plots the light gray area indicates the school closure, and the hatched gray area represents the regular school holiday.
In the top (bottom) row, the school closure is triggered in late (early) spring, resulting in maximally increased (decreased) final size.

of year when $\beta(t)$ is falling, may not reduce the stock of susceptible individuals sufficiently to prevent the epidemic from forming a second wave in the autumn, during a favorable time of year when $\beta(t)$ begins to rise again. A model with the same parameters, except for a different time of introduction of the virus to the population, could exhibit only a winter or spring peak of infection if that peak was large enough to reduce the stock of susceptible individuals sufficiently by the end of the summer to prevent a second autumn wave of infection from occurring. The underlying reason for the increase in pandemic final size when school closures occur in late spring is related to these non-linear dynamics.

Spring school closures essentially increase the stock of susceptible individuals in the population at the end of the summer, and if the epidemic is still ongoing by that point (even at a low level), this larger stock of susceptible individuals can act

as tinder for the pandemic to continue in the more favorable influenza season of autumn, resulting in a larger overall final size than might have occurred if school closures had not been implemented (up to 20% larger for a school closure that occurs in late spring). However, late spring school closures have the advantage that the average time of the peak is shifted by up to two months, possibly allowing enough time for development of vaccines to mitigate the larger size of the epidemic; school closures in the seasonally forced model always delay the average time of the peak, although if the school closure occurs too close to the peak time (which occurs for a high prevalence trigger threshold), the delay is not significant.

In our studies we examined scenarios involving various prevalence fractions used to trigger the school closure. Prior to 2009, few states in the U.S. had official pandemic school closure policies, but those that did employed remarkably high school absentee thresholds, from 10% to 30%[21, 22]. We observed that the only pandemics in our study that met the 10% prevalence trigger threshold were pandemics that peaked in winter, and that while a 4 week school closure triggered by this threshold did in fact have noticeable impact on the final size of the pandemic, reducing it by a relative factor of almost 10%, it had virtually no impact on the timing or width of the peak. Very low prevalence thresholds of 0.1% tended to have significant positive impact on the final size and peak width and timing only for early spring pandemics. More moderate prevalence triggers of around 1% appeared to perform the best, reducing the final size with a 4 week school closure during winter pandemics just as much as a closure triggered by a 10% trigger. The 1% trigger also appeared to carry lower risk of negatively impacting the final size of the pandemic compared to the 0.1% trigger, as long as it was not applied just before the summer holidays.

In summary, our model studies suggest that when a disease exhibits periodic patterns in transmission, decisions of public health policy will be particularly important as to how control measures, such as school closures, should be implemented. Our studies underline that it is important to simultaneously consider various figures of merit when making these decisions (such as timing of the closure, length of the closure, and the prevalence threshold triggering the closure). Mathematical models, such as the ones we have implemented here, can be helpful for understanding these complex disease transmission dynamics, and can be useful for identifying optimal control strategies.

Acknowledgments. This research is partially supported by NSF grants DMS-0719697 and DMS-1022758.

REFERENCES

[1] W. J. Alonso, C. Viboud, L. Simonsen, E. W. Hirano, L. Z. Daufenbach and M. A. Miller, *Seasonality of influenza in Brazil: A traveling wave from the Amazon to the Subtropics,* Am. J. Epidemiol., **165** (2007), 1434–1442.

[2] R. Anderson and R. M. May, "Infectious Diseases of Humans: Dynamics and Control," Oxford University Press, New York, 1991.

[3] N. Bacaër and E. H. Ait Dads, *Genealogy with seasonality, the basic reproduction number, and the influenza pandemic,* J. Math. Biol., **62** (2011), 741–762.

[4] N. Bacaër and M. G. M. Gomes, *On the final size of epidemics with seasonality*, Bulletin of Mathematical Biology, **71** (2009), 1954–1966.

[5] N. Bacaër, *Approximation of the basic reproduction number R_0 for vector-borne diseases with a periodic vector population,* Bull. Math. Biol., **69** (2007), 1067–1091.

[6] N. Bacaër and S. Guernaoui, *The epidemic threshold of vector-borne diseases with seasonality,* J. Math. Biol., **53** (2006), 421–436.
[7] S. Cauchemez, N. M. Ferguson, C. Wachtel, A. Tegnell, G. Saour, B. Duncan and A. Nicoll, *Closure of schools during an influenza pandemic,* Lancet. Infect. Dis., **9** (2009), 473–481.
[8] S. Cauchemez, A.-J. Valleron, P.-Y. Boëlle, A. Flahault and N. M. Ferguson, *Estimating the impact of school closure on influenza transmission from Sentinel data,* Nature, **452** (2008), 750–754.
[9] V. Colizza, A. Barrat, M. Barthelemy, A.-J. Valleron and A. Vespignani, *Modeling the worldwide spread of pandemic influenza: Baseline case and containment interventions,* PLoS Med., **4** (2007), e13.
[10] S. Y. Del Valle, P. D. Stroud and S. M. Mniszewski, *Dynamic contact patterns and social structure*, in "Realistic Social Networks in Social Networks: Development, Evaluation, and Influence," Nova Science Publishers, (2009), 201–216.
[11] S. F. Dowell, *Seasonal variation in host susceptibility and cycles of certain infectious diseases*, Emerg. Infec. Dis., **7** (2001), 369–374.
[12] J. Dushoff, J. B. Plotkin, C. Viboud, D. J. Earn and L. Simonsen, *Mortality due to influenza in the United States*, American Journal of Epidemiology, **163** (2006), 181–187.
[13] Z. Feng, S. Towers and Y. Yang, *Modeling the effects of vaccination and treatment on pandemic influenza*, American Association of Pharmaceutical Science Journal, **13** (2011), 427–437.
[14] N. M. Ferguson, D. A. T. Cummings, C. Fraser, J. C. Cajka, P. C. Cooley and D. S. Burke, *Strategies for mitigating an influenza pandemic,* Nature, **442** (2006), 448–452.
[15] N. M. Ferguson, A .P. Galvani and R. M. Bush, *Ecological and immunological determinants of influenza evolution,* Nature, **422** (2003), 428–433.
[16] C. Fraser, *et al.*, *Pandemic potential of a strain of influenza A(H1N1): Early findings,* Science, **324** (2009), 1557–1561.
[17] T. C. Germann, K. Kadau, I. M. Longini and C. A. Macken, *Mitigation strategies for pandemic influenza in the United States,* PNAS, **103** (2006), 5935–5940.
[18] R. J. Glass, L. M. Glass, W. E. Beyeler and J. H. Min, *Targeted social distancing design for pandemic influenza,* Emerg. Infect. Dis., **12** (2006), 1671–1681.
[19] M. Z. Gojovic, B. Sander, D. Fisman, M. D. Krahn and C. T. Bauch, *Modelling mitigation strategies for pandemic (H1N1) 2009,* CMAJ, **181** (2009), 673–680.
[20] N. Halder, J. Kelso and G. Milne, *Analysis of the effectiveness of interventions used during the 2009 A/H1N1 influenza pandemic,* BMC Public Health, **10** (2010), 168.
[21] S. D. Holmberg, C. M. Layton, G. S. Ghneim and D. K. Wagener, *State plans for containment of pandemic influenza,* Emerg. Infect. Dis., **12** (2006), 1414–1417.
[22] L. Kahn, *Pandemic influenza school closure policies,* Emerg. Infect. Dis., **13** (2007), 344–345.
[23] J. K. Kelso, G. J. Milne and H. Kelly, *Simulation suggests that rapid activation of social distancing can arrest epidemic development due to a novel strain of influenza,* BMC Public Health, **9** (2009).
[24] B. Y. Lee, S. T. Brown, P. Cooley, M. A. Potter, W. D. Wheaton, R. E. Voorhees, S. Stebbins, J. J. Grefenstette, S. M. Zimmer, R. K. Zimmerman, T. M. Assi, R. R. Bailey, D. K. Wagener and D. S. Burke, *Simulating school closure strategies to mitigate an influenza epidemic,* Journal of Public Health Management and Practice, **16** (2010), 252–261.
[25] E. Lofgren, N.H . Fefferman, Y. N. Naumov, J. Gorski and E. N. Naumova, *Influenza seasonality: Underlying causes and modeling theories,* J. Virol., **81** (2007), 5429–5436.
[26] A. C. Lowen, S. Mubareka, J. Steel and P. Palese, *Influenza virus transmission is dependent on relative humidity and temperature,* PLoS Pathogens, **4** (2007), 151–158.
[27] J. Medlock and A. P. Galvani, *Optimizing influenza vaccine distribution*, Science, **325** (2009), 1705–1708.
[28] G. J. Milne, J. K. Kelso, H. A. Kelly, S. T. Huband and J. McVernon, *A small community model for the transmission of infectious diseases: Comparison of school closure as an intervention in individual-based models of an influenza pandemic,* PLoS ONE, **3** (2008), e4005.
[29] J. Mossong, N. Hens, M. Jit, P. Beutels, K. Auranen, R. Mikolajczyk, M. Massari, S. Salmaso, G. Scalia Tomba, J. Wallinga, J. Heijne, M. Sadkowska-Todys, M. Rosinska and W. J. Edmunds, *Social contacts and mixing patterns relevant to the spread of infectious diseases,* PLoS Med, **5** (2008), e74.

[30] B. Sander, A. Nizam, L. P. Garrison, M. J. Postma, M. E. Halloran and I. M. Longini, *Economic evaluation of influenza pandemic mitigation strategies in the United States using a stochastic microsimulation transmission model,* Value in Health, **12** (2009), 226.
[31] S. Towers and Z. Feng, *Pandemic H1N1 influenza: Predicting the course of pandemic and assessing the efficacy of the planned vaccination programme in the United States,* Eurosurveillance, **14** (2009).
[32] S. Towers, K. Vogt Geisse, Y. Zheng and Z. Feng, *Antiviral treatment for pandemic influenza: Assessing potential repercussions using a seasonally forced SIR model,* Journal of Theoretical Biology, **289** (2011), 259–268.
[33] U.S. 2000 Census. Available from: http://www.census.gov.
[34] W. Wang and X.-Q. Zhang, *Threshold dynamics for compartmental epidemic models in periodic environments*, J. Dyn. Diff. Equat., **20** (2008), 699–717.
[35] World Health Organization, *Nonpharmaceutical interventions for pandemic influenza, national and community measures,* Emerg. Infec. Dis., **12** (2006), 88–94.
[36] Y. Yang, Jonathan D. Sugimoto, M. E. Halloran, N. E. Basta, D. L. Chao, L. Matrajt, G. Potter, E. Kenah and I. M. Longini Jr., *The transmissibility and control of pandemic influenza A(H1N1) virus,* Science, **326** (2009), 729–733.

Received June 20, 2011; Accepted November 3, 2011.

E-mail address: stowers@purdue.edu
E-mail address: kvogtgei@math.purdue.edu
E-mail address: tsai3@purdue.edu
E-mail address: han85@purdue.edu
E-mail address: zfeng@math.purdue.edu